Test of Reaction Kinetics Using Both Differential Scanning and Accelerating Rate Calorimetries As Applied to the Reaction of Li_xCoO_2 in Non-aqueous Electrolyte

D. D. MacNeil[†] and J. R. Dahn*[,†,‡]

Department of Chemistry, Dalhousie University, Halifax, Nova Scotia, B3H3J5, Canada, and Department of Physics, Dalhousie University, Halifax, Nova Scotia, B3H3J5, Canada

Received: March 29, 2000; In Final Form: February 27, 2001

Extracting reliable reaction kinetics from nonisothermal calorimetric results can be difficult. The reaction model, activation energy, and frequency factor make up a "kinetic triplet" for a particular reaction and define the reaction kinetics. One expects a good correlation between data and the predictions of the reaction model for a variety of experiments, provided the reaction triplet has been well determined. Such a correlation is expected for the results of accelerating rate calorimeter (ARC) and differential scanning calorimeter (DSC) experiments. As an example, the reaction of Li_xCoO_2 in nonaqueous electrolyte (as is important in Li-ion battery safety) has been studied with both DSC and ARC. Comparing the shape of ARC profiles to those predicted theoretically limits the choice of reaction model. The activation energy is determined from the shift of the DSC profile with heating rate or from the change in the initial self-heating rate of ARC samples as a function of temperature. The frequency factor is then chosen to give the correct DSC peak temperature and correct self-heating rate. Calculated DSC and ARC curves fit experiment well for several related reaction models.

Introduction

When a reactant is converted to products by a single-step thermally induced reaction, it is common to write

$$\frac{d\alpha}{dt} = k(T)f(\alpha) \tag{1}$$

where t is the time, T is the temperature, and α is the fractional degree of conversion of reactants ($0 \le \alpha \le 1$). It is common to assume that the temperature dependence of the rate constant $k(T)$ can be separated from the reaction model, $f(\alpha)$, and that

$$k(T) = \gamma e^{-(E_a/k_B T)} \tag{2}$$

where E_a is the activation energy, k_B is Boltzmann's constant, and γ is the frequency factor. The reaction model, $f(\alpha)$, can be derived for a number of physical situations and examples are given in Table 1.[1] To describe the reaction kinetics accurately, it is necessary to determine the "kinetic triplet", $f(\alpha)$, E_a and γ.

The determination of reaction kinetics from nonisothermal methods such as differential scanning calorimetry (DSC) is well-known.[1,2] However, significant care must be taken to ensure that the kinetic triplet obtained from an analysis of results is meaningful.[3,4] In some studies, the kinetic triplet has been determined by fitting (optimizing activation energy and frequency factor) alternative reaction models to a single or a series of differential scanning calorimeter (DSC) or thermal gravimetric analysis (TGA) experiments. The kinetic triplet giving the lowest residual is then selected as representative of the reaction, even though other reaction models may give fits of slightly higher residual and values of activation energy and frequency factor that can be different by a factor of 4 and several orders of magnitude, respectively. For example, Vyazovkin and Wight[3] show that fitting models to experiment can lead to a variation in E_a and $\ln(\gamma)$ of a factor of 4, depending on the model chosen, with little change in the residual of the fit (see Table 3 in ref 3). They go on to show that confidence in the determined reaction model can be obtained when combinations of isothermal and nonisothermal results are treated with an isoconversional

TABLE 1: Reaction Models Typically Applied to Describe the Thermal Decomposition of Solids

			$k\alpha^m(1-\alpha)^n(-\ln(1-\alpha))^p$		
	reaction model	$d\alpha/dt =$	m	n	P
1	one-dimensional diffusion	$k\alpha^{-1}$	−1	0	0
2		$k\alpha$	1	0	0
3	power law	$k\alpha^{1/2}$	0.5	0	0
4	power law	$k\alpha^{2/3}$	2/3	0	0
5	power law	$k\alpha^{3/4}$	3/4	0	0
6	zero order	k	0	0	0
7	contracting cylinder	$k(1-\alpha)^{1/2}$	0	0.5	0
8	contracting sphere	$k(1-\alpha)^{2/3}$	0	2/3	0
9	first order (n^{th} order)	$k(1-\alpha)$	0	1	0
10	second order (n^{th} order)	$k(1-\alpha)^2$	0	2	0
11	Avrami−Erofeev	$k(1-\alpha)(-\ln(1-\alpha))^{1/2}$	0	1	0.5
12	Avrami−Erofeev	$k(1-\alpha)(-\ln(1-\alpha))^{2/3}$	0	1	2/3
13	Avrami−Erofeev	$k(1-\alpha)(-\ln(1-\alpha))^{3/4}$	0	1	3/4
14	autocatalytic	$k\alpha(1-\alpha)$	1	1	0
15	two-dimensional diffusion	$k(-\ln(1-\alpha))^{-1}$	0	0	−1
16	diffusion controlled	$k(1-(1-\alpha)^{1/3})^{-1}(1-\alpha)^{2/3}$			
17	diffusion controlled	$k((1-\alpha)^{-1/3}-1)^{-1}$			

* To whom correspondence should be addressed. Phone: 902-494-2312. Fax: 902-494-5191. E-mail: jeffdahn@is.dal.ca.
† Department of Chemistry, Dalhousie University.
‡ Department of Physics, Dalhousie University.

10.1021/jp001187j CCC: $20.00
Published on Web 04/12/2001

method. The kinetic treatment of adiabatic data, such as that collected in accelerating rate calorimetry, usually involves the assumption of a kinetic model to determine the kinetic parameters,[5] but again, these values may produce the incorrect behavior under a variety of conditions. New methods have been developed, such as in ref 6, but their discrimination among kinetic models is not very effective (see Figures 7 and 8 in ref 6).

Commonly, the kinetic analyses of DSC profiles are performed with methods derived from those traditionally assigned to Ozawa[7] and Kissinger.[8] Although theses methods can provide a kinetic triplet for the process under study, the correct selection for the reaction model ($f(\alpha)$) is based on a plot of experimental data in a particular fashion. In the end, the correct kinetic triplet is based on the agreement between the experimental and the calculated profiles using statistics. The difficulty with determining the reaction triplet in this fashion is that the parameters are often determined under a limited range of experimental conditions, and thus, significant care must be used when extrapolating the kinetic triplet to unexplored reaction conditions. What is required is an experimental method that probes the reactions over a widely varying temperature regime and a kinetic triplet that can fit all these experiments satisfactorily.

It is our opinion that much of the difficulty in selecting the appropriate reaction model is that the shape of DSC profiles is not strongly dependent on the choice of reaction model. In particular, a single DSC trace of a single-step reaction can always be fitted quite closely for most choices of $f(\alpha)$, provided that the choice of E_a and γ is arbitrary. If several DSC experiments are available at very different sweep rates, then the kinetic triplet can be more tightly determined[3]. Selecting kinetic parameters and models from the analysis of DSC peak shapes has been reviewed elsewhere (see Biader Ceipidor et al. and references therein[9]), but again, the selection of the most suitable kinetic triplet is often determined by the fit to experiment with the smallest sum of residuals.

In this paper, we show that the shape of accelerating rate calorimeter (ARC) profiles (self-heating rate versus temperature) is very sensitive to the choice of $f(\alpha)$. This has been discussed by Sempere et al.[10] for a limited number of functions of $f(\alpha)$ (see Figure 3 in ref 10). Accelerating rate calorimetry has a number of advantages over DSC analysis because the ARC has a detection limit of 0.02 K/min that effectively corresponds to a sweep rate that is 50 times lower than conveniently obtainable by DSC. This lower effective sweep rate gives rise to a much larger range, over which exothermic reactions can be analyzed and the reaction triplet tested. Thus, including ARC results in any kinetic analysis allows for a stringent test on any possible model proposed. If DSC results at several sweep rates and ARC profiles for a number of different start temperatures can be fit with a single kinetic triplet, then confidence in the description of the reaction is assured. This will give confidence in predicting the outcome of other unexplored reaction conditions (such as thermal modeling of batteries exposed to elevated temperatures). We illustrate our procedure with studies of the reaction of Li_xCoO_2 with nonaqueous electrolyte, as would be found in a lithium-ion cell under thermal abuse.

Lithium-ion batteries are used in laptop computers, cellular phones, and other portable electronic equipment. This technology has always been subject to strict safety regulations for application in consumer products because it is well-known[11,12] that the charged electrodes react with the electrolyte in the cells under conditions of severe electrical or thermal abuse. Lithium-ion battery researchers currently use a variety of techniques such as DSC,[13] thermal gravimetric analysis (TGA)[14] and ARC[15,16,17] to study the reactions occurring at elevated temperatures.

Our laboratory has pioneered the analyses of the electrode/electrolyte reactions using ARC.[15,16,17] The ARC is an adiabatic calorimeter.[18] In our work, a charged electrode (0.35 g) and electrolyte (0.35 g) are hermetically sealed in a thin-walled stainless steel tube (0.9 g) by Tungsten Inert Gas (TIG) welding to make a sample for ARC analysis. The sample is mounted on a thermocouple at the center of the ARC chamber. The walls of the ARC heat the sample to a target temperature at a rapid rate (usually 5 K/min) and the sample comes to equilibrium there. If an exotherm is detected (self-heating of the sample greater that 0.02 K/min) then the calorimeter walls match the sample temperature and follow the exotherm as it occurs. If no exotherm is detected, the calorimeter increases the target temperature in a series of steps. Since the sample and the calorimeter walls are at almost the same temperature during the exotherm, the exotherm is monitored under quasi-adiabatic conditions.

We have learned the importance of doing numerous ARC experiments on nominally identical samples. We use the first experiment to find the temperature of the exotherm at our detection limit and follow it to completion. Subsequent experiments on fresh samples are initially forced to temperatures above the initial onset of the exotherm. Provided that the heating rate of the ARC to the target (5 K/min) is much larger than the initial self-heating rate of the sample at the target temperature, we can then assume $f(\alpha)$ in eq 1 has approximately the same value for all the samples at the start of their exotherms. Because the self-heating rate dT/dt is proportional to $d\alpha/dt$, we can use an Arrenhius plot ($\log(dT/dt)$ versus $1/T$) of the initial self-heating rates at various temperatures to determine E_a and $\gamma f(\alpha_0)$, where α_0 is the initial value of α at the start of the reaction. We then use the shape of the dT/dt versus T plots, the ARC profiles, to assist in the selection of the reaction model. Once $f(\alpha)$ is determined, then one can solve for γ.

DSC results are then used to test the kinetic triplet obtained. Generally, the obtained kinetic triplet can model the DSC results approximately, without severe adjustment. However, the temperature dependence of the DSC peak position and the shape and width of the DSC peaks can be used to "fine tune" the kinetic triplet obtained from ARC. Finally, a complete simultaneous least-squares fit of the kinetic model to a number of DSC runs at different sweep rates and a number of ARC runs at different starting temperatures is made, to optimize the kinetic triplet. In this paper, we show how the results of both ARC and DSC experiments agree well with the predictions of a single kinetic triplet for the reaction of Li_xCoO_2 in electrolyte. In addition, we show that DSC experiments on Li_xCoO_2 in electrolyte must have analysis conditions controlled very carefully, or else irreproducible results can be obtained.

Calculated ARC and DSC Profiles for Various Choices of $f(\alpha)$. In an ARC experiment, the self-heating rate is given by

$$\frac{dT}{dt} = \frac{h}{C_{tot}} * \frac{d\alpha}{dt} \tag{3}$$

where h is the total heat which can be evolved by the sample due to the reaction (Joules) and C_{tot} is the total heat capacity of the reactants and the stainless steel tube (JK^{-1}). h/C_{tot} corresponds to the temperature rise, ΔT, from the onset of the

TABLE 2: Parameters Used to Calculate ARC and DSC Profiles for the Reaction Models of Table 1

reaction model	E_a (eV)	γ (min^{-1})	α
1	1.6	5×10^{15}	0.001
2	1.6	5×10^{18}	0.001
3	1.6	5×10^{17}	0.001
4	1.6	5×10^{17}	0.001
5	1.6	8×10^{17}	0.001
6	1.6	5×10^{16}	0.001
7	1.6	5×10^{16}	0.001
8	1.6	5×10^{16}	0.001
9	1.6	5×10^{16}	0.001
10	1.6	5×10^{16}	0.001
11	1.6	5×10^{17}	0.001
12	1.6	5×10^{17}	0.001
13	1.6	5×10^{17}	0.001
14	1.6	5×10^{18}	0.001
15	1.6	5×10^{15}	0.001
16	1.6	5×10^{15}	0.001
17	1.6	5×10^{15}	0.001

exotherm to the end of the first exothermic behavior because

$$\int_0^\infty \frac{dT}{dt} = \Delta T \tag{4}$$

and

$$\int_0^\infty \frac{h}{C_{tot}} \frac{d\alpha}{dt} dt = \frac{h}{C_{tot}} \Delta\alpha = \frac{h}{C_{tot}} \tag{5}$$

Since $\Delta\alpha = 1$ for the complete consumption of the reactant, thus

$$\Delta T = \frac{h}{C_{tot}}$$

For the experiments to be described later, ΔT was found to be about 60 K.

In a DSC experiment, the generated power is

$$P = H\, d\alpha/dt \tag{6}$$

where H is the total heat generated by the reaction per gram of reactant, and α and t are as described above. For the experiments to be described later, H was found to be about 265 J/g.

To compare ARC and DSC calculations for various reaction models, we made the following restrictions. First, we selected E_a to be 1.6 eV, which is close to experiment, as we will see below. Next, we selected γ so that the ARC simulation would produce measurable self-heating at 140 °C. Finally, we selected $\alpha_0 = 0.001$ for most simulations. Table 2 lists the values of the parameters used for the simulations of the reaction models given in Table 1.

The reaction models given in Table 1 are those typically used to describe the thermal decomposition of solids. The Table contains a column for the reaction model type, a column for the differential equation describing the extent of conversion and columns used to describe exponents in a "universal" equation for the thermal decomposition of solids[1]

$$\frac{d\alpha}{dt} = k\alpha^m(1-\alpha)^n(-ln(1-\alpha))^p \tag{7}$$

The variables in eq 7 can be chosen to describe most solid thermal decomposition mechanisms from simple n^{th}-order to diffusion-controlled reactions.

The ARC and DSC profiles for a typical zero-order reaction are shown in Figure 1. The start points for the ARC calculations

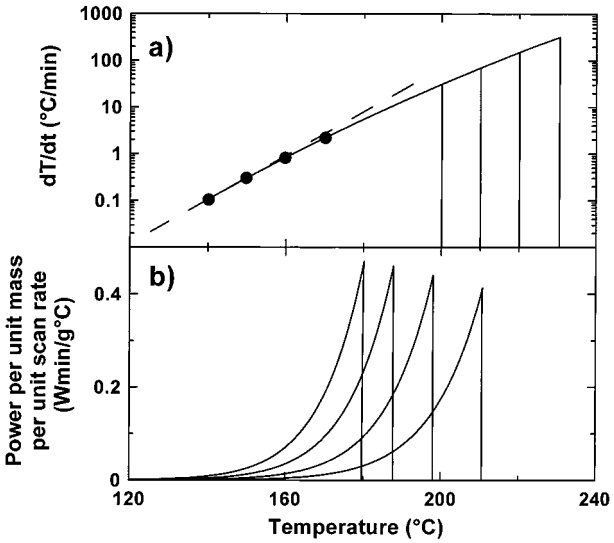

Figure 1. Calculated (a) ARC and (b) DSC profiles for zero order kinetics (model 6 in Table 1) using the parameters for model 6 in Table 2. The large circles in (a) indicate the start point of the ARC calculations. A value of $h/C_{tot} = 60$ K was used in (a) and $H = 270$ J/g in(b). The scan rates in (b) were 1, 2, 5, and 15 K/min.

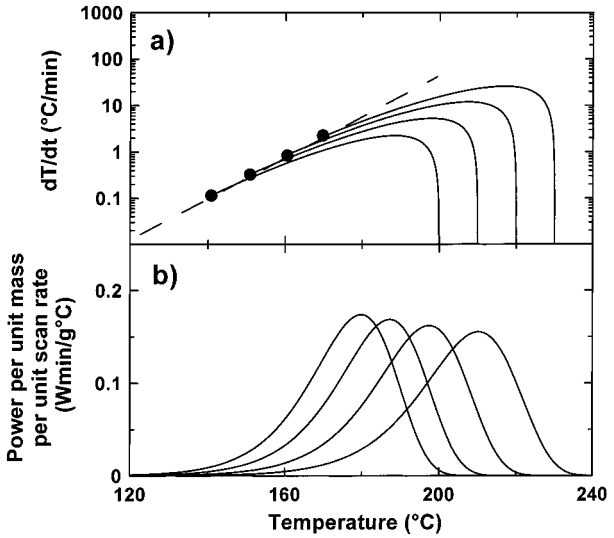

Figure 2. Calculated (a) ARC and (b) DSC profiles for first-order kinetics (model 9 in Table 1) using the parameters for model 9 in Table 2. The large circles in (a) indicate the start point of the ARC calculations. A value of $h/C_{tot} = 60$ K was used in (a) and $H = 270$ J/g in (b). The scan rates in (b) were 1, 2, 5, and 15 K/min. The dashed line in (a) is the "Arhennius line" described in the text.

were 140, 150, 160, and 170°C, and the DSC sweep rates were 1, 2, 5, and 15 K/min. In a zero-order reaction, the consumption of reactants does not affect the reaction rate until they are completely consumed ($\alpha = 1$), thus both DSC and ARC profiles increase until they abruptly stop. The dashed line through the start points of the ARC experiments is called the "Arrhenius line" here because these points would be used in an Arrhenius plot to determine E_a.

Figure 2 shows ARC and DSC profiles for a first-order reaction. The DSC curves display a bell-shaped appearance, whereas the ARC profile deviates to the right of the "Arrhenius line". If the order of the reaction is increased (e.g., model 10 in Table 1), then the shapes of the DSC and ARC profiles remain approximately the same, with the exception that the DSC trace becomes broader (half width increases) and the ARC trace has a greater deviation from the "Arrhenius line". If the order of

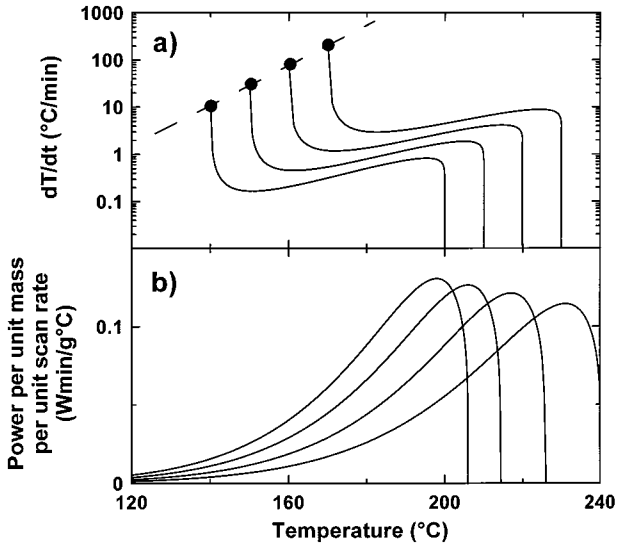

Figure 3. Calculated (a) ARC and (b) DSC profiles for diffusion-controlled kinetics (model 15 in Table 1) using the parameters for model 15 in Table 2. The large circles in (a) indicate the start point of the ARC calculations. A value of $h/C_{tot} = 60$ K was used in (a) and $H = 270$ J/g in (b). The scan rates in (b) were 1, 2, 5 and 15 K/min. The dashed line in (a) is the "Arhennius line" described in the text.

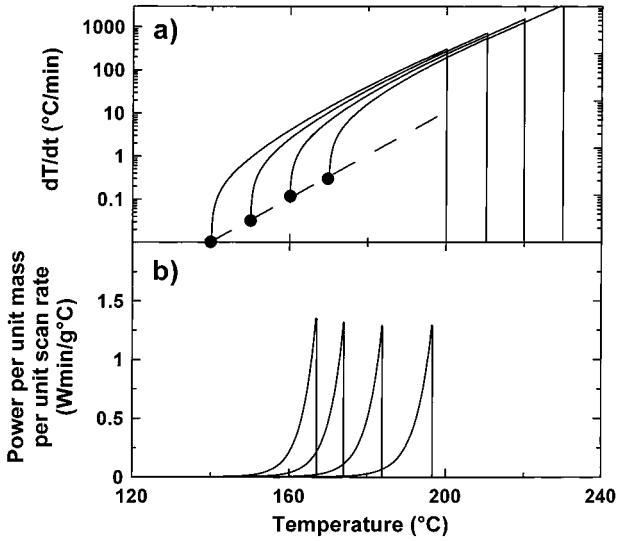

Figure 4. Calculated (a) ARC and (b) DSC profiles for power-law kinetics (model 4 in Table 1) using the parameters for model 3 in Table 2. The large circles in (a) indicate the start point of the ARC calculations. A value of $h/C_{tot} = 60$ K was used in (a) and $H = 270$ J/g in (b). The scan rates in (b) were 1, 2, 5, and 15 K/min. The dashed line in (a) is the "Arhennius line" described in the text.

the reaction is decreased (model 7 in Table 1), then the shapes of the DSC and ARC profiles remain approximately the same, with the exception that the DSC trace becomes narrower (half width decreases) and the ARC trace lies closer to the "Arrhenius line"

Figure 3 shows the typical profiles that would be obtained in a reaction governed by diffusion (model 15 in Table 1). These reactions have their overall rate governed by the movement of one or more reactant species to, or a product from, a reaction interface. The ARC profile is easily distinguishable from n^{th}-order reaction kinetics since it has a high initial self-heating rate that then rapidly decreases followed by a region of approximately constant increasing slope. On the other hand, the DSC profile increases slowly from low temperature and then

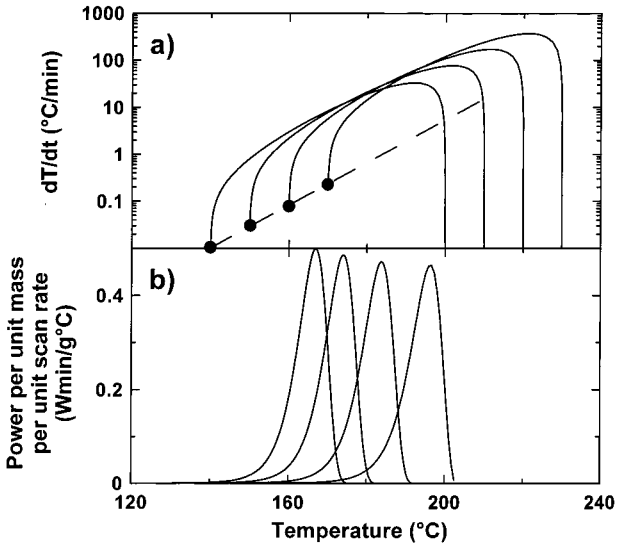

Figure 5. Calculated (a) ARC and (b) DSC profiles for Avrami−Erofeev kinetics (model 12 in Table 1) using the parameters for model 12 in Table 2. The large circles in (a) indicate the start point of the ARC calculations. A value of $h/C_{tot} = 60$ K was used in (a) and $H = 270$ J/g in (b). The scan rates in (b) were 1, 2, 5, and 15 K/min. The dashed line in (a) is the "Arhennius line" described in the text.

falls off fairly rapidly after the peak in the trace in a manner not so different from zero order kinetics.

Figure 4 shows the ARC and DSC profiles for a reaction governed by power law kinetics (model 4 in Table 1). Power law kinetics are obtained when the initial growth of nuclei is slower than the constant value that is subsequently attained[1]. The DSC profile is similar to that of a zero-order reaction as can be seen by comparing to Figure 1. The ARC profile lies to the left (above) of the "Arrhenius line" indicating that the reaction is accelerated by the presence of product. This is seen by the rapid initial rise in self-heating rate that then levels to an approximately constant upward slope, which continues until the reaction is complete. The ARC profile is easily distinguished from those previously shown.

Figure 5 shows the ARC and DSC profiles for an Avrami−Erofeev reaction (model 12). The Avrami−Erofeev expressions have been found to describe many solid-phase decompositions, phase transformations, recrystallizations and reactions between solids.[1] The DSC profile has a peak shape similar to an n^{th}-order reaction, except that the peak width is smaller. The ARC profile lies to the left (above) the "Arrhenius line" with an increasing self-heating rate but then decreases smoothly when the reactant begins to run out.

So far, the value of α_0 in all the simulations has been set to 0.001. Figure 6 shows the dependence of a typical ARC profile for an Avrami−Erofeev reaction (model 12 in Table 1) on the initial choice of α_0. As the value of α_0 increases, the initial rise in the self-heating rate is reduced. Figure 7 shows the dependence of the DSC profile on α_0 for the same reaction model. As α_0 increases, the peak width of the DSC trace increases, although the effect is small for $\alpha_0 < 0.02$. If α_0 is treated as an adjustable parameter during modeling of reactions, then it is clear that fits to ARC profiles can help to extract it.

Calculations of ARC and DSC traces for the other models in Table 1 are similar to one of Figures 1−5. It is our opinion that the changes in the ARC profiles with reaction model are more profound than the changes seen in DSC. In any event, the combination of studies by both ARC and DSC should lead

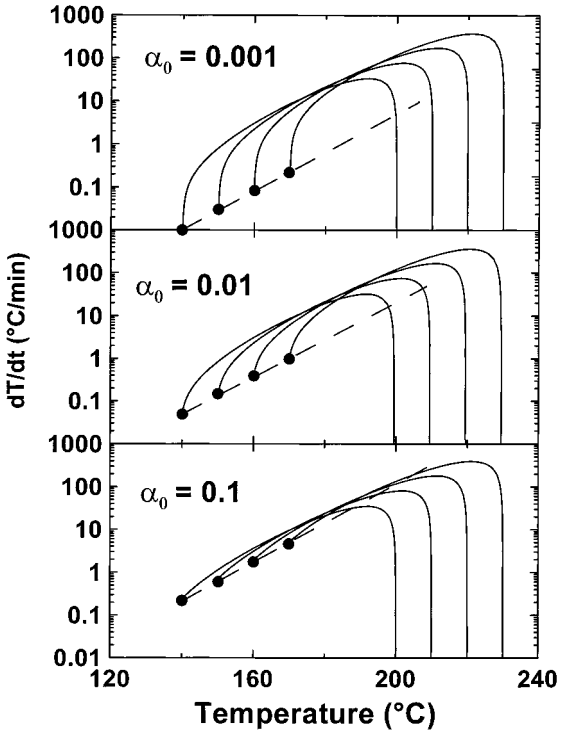

Figure 6. Calculated ARC profiles based on the model and parameters used in Figure 5, except for values of α_0 as indicated.

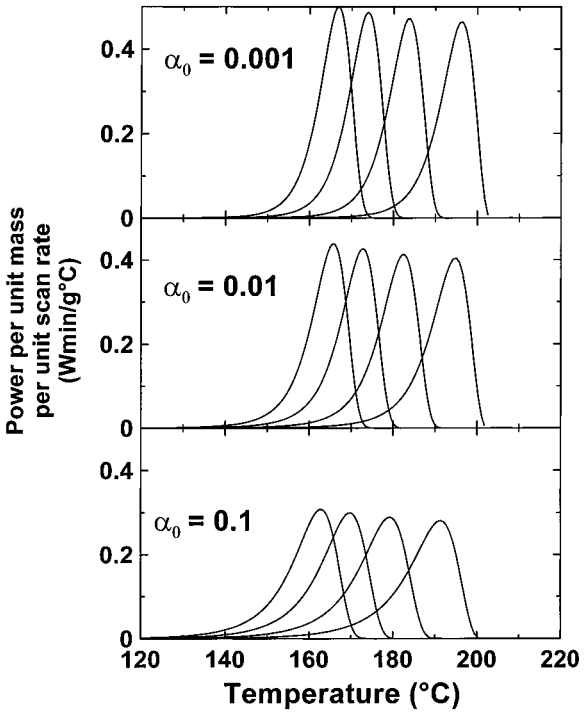

Figure 7. Calculated DSC profiles based on the model and parameters used in Figure 5, except for values of α_0 as indicated.

to a more reliable determination of kinetic triplets. We now attempt to illustrate this with our studies on Li_xCoO_2 in electrolyte.

Experimental Section

$LiCoO_2$ was obtained from E-One Moli/Energy Canada Ltd (Vancouver, B.C.). It had lattice constants $a = 2.8141$ Å and $c = 14.0436$ Å, and a BET surface area of 0.11 m^2/g. Samples of Li_xCoO_2 were prepared in standard 2325 coin cell hardware in a true lithium-ion configuration, that is, a $LiCoO_2$ (FMC) cathode and an MCMB (Osaka Gas) carbon anode, to simulate conditions of true commercial batteries, as described previously.[15] Electrodes were prepared by combining 7%, by mass, each of Super S Carbon Black (MMM Carbon, Belgium) and poly(vinylidene difluoride) (PVDF, 10% in *N*-methyl pyrolidinone (NMP), NRC) with the electrode powders. The amount of MCMB used was ~300 mg, whereas the amount of $LiCoO_2$ used was ~750 mg. The pellets were about 18 mm in diameter and each was about 1 mm thick. Assuming a first discharge capacity of about 350 mAh/g for the carbon and a reversible capacity of about 140 mAh/g for the $LiCoO_2$ at 4.2 V, these masses lead to a coulometrically balanced cell.

The electrodes were then transferred to an argon filled glovebox and cell construction proceeded as before.[15] 1M $LiPF_6$ in ethylene carbonate (EC): diethyl carbonate (DEC) (33:67) electrolyte (Mitsubishi Chemicals) was used as electrolyte and three polypropylene #2502 separators (Celanese) were used. The cells were first charged to 4.2 V, with a current of 1.0 mA. After obtaining 4.2 V the cells were cycled twice between 2.5 and 4.2 V. After cycling, a signature-charge test (equivalent to constant voltage charging) was used to stabilize the electrode at the desired voltage. The coin cells were then transferred to an argon-filled glovebox where construction of the ARC and DSC samples was done. The DSC samples (2−7 mg) were placed and sealed into hermetic aluminum DSC cans in the argon-filled glovebox. No additional electrolyte was added. The DSC measurement were performed at a variety of heating rates starting from room temperature using a DuPont 910 differential scanning calorimeter. For the ARC samples, the Li_xCoO_2 powder (0.35 g) was placed in a stainless steel tube with an equal amount of excess electrolyte added, and the tube was then sealed by TIG welding in the glovebox. The sample was then analyzed in the ARC.

Comparison of the predictions of model kinetic triplets to experiment was made by least-squares analysis. Goodness of fit parameters, χ^2, for the fits to ARC and DSC results are defined here as follows

$$\chi^2_{ARC} = \frac{1}{N}\sum_{n=1}^{N}\frac{[dT/dt_{expt} - dT/dt_{calc}]^2}{dT/dt_{expt}} \quad (8)$$

$$\chi^2_{DSC} = \frac{10}{N}\sum_{n=1}^{N}\frac{[H_{expt} - H_{calc}]^2}{H_{expt}} \quad (9)$$

and

$$\chi^2_{tot} = \chi^2_{ARC} + \chi^2_{DSC} \quad (10)$$

A 10 times weighting factor (see above in eq 9) was given to the DSC results because the numerical values of the power per gram per sweep rate were on average about 10 times smaller than the self-heating rates in the ARC. With this procedure, fit quality to ARC and to DSC was given about equal overall weight. Fits were made to individual experiments and in addition one fit was made simultaneously to the results of six experiments: DSC runs at sweep rates of 1, 2, 5 and 15 K/min and ARC runs starting at 160 and 170 °C.

Results and Discussion

In a previous paper,[15] we reported that the initial reaction of Li_xCoO_2 at elevated temperature followed an autocatalytic

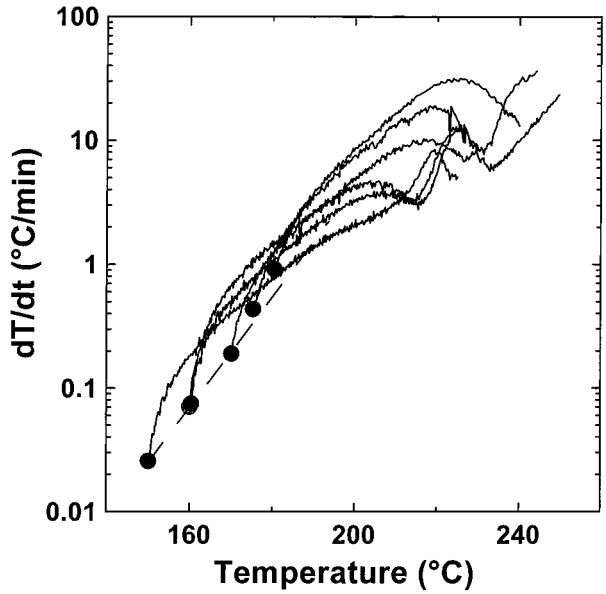

Figure 8. ARC experiments on Li_xCoO_2 in electrolyte. The large dots indicate the start point of each experiment. The dashed line is the "Arhennius line" described in the text.

mechanism, whereby the reaction is accelerated by the presence of products. The self-heating profiles for Li_xCoO_2 in electrolyte are shown in Figure 8, where the start points of identical samples are indicated by the large circles. It is clear that the majority of the ARC profiles lie to the left (above) the Arhennius line. A simple model was proposed to describe this behavior based on that given by Grewer,[19] using a modified Sestak-Berggren equation (eq 10). The proposed model reproduced the behavior seen in the initial decomposition of Li_xCoO_2. Grewer's model is based on the following differential equation

$$\frac{d\alpha}{dt} = k(1-\alpha)(\beta + \alpha^{0.5}) \qquad (11)$$

where β is the parameter of autocatalysis. This is approximately equivalent to eq 7 if $\alpha_0 = \beta^2$, $m = 0.5$, $n = 1$ and $p = 0$. If $\alpha = 0$ in eq 11, the autocatalytic reaction has not been initiated and a high degree of autocatalysis implies a small value of β.

In ref 15, the parameters were chosen by "eye" such that the model reproduced the behavior seen in the initial decomposition of all the experimental results for Li_xCoO_2. An activation energy of 1.6 eV was chosen and with the corresponding frequency factor of 1.9×10^{16} min^{-1} the behavior was qualitatively reproduced. In this work, an optimized fit to the experimental ARC data (collected at 160 °C and 170 °C) was obtained and the ARC profile is shown in Figure 9. The initial kinetic values were obtained through an Arrhenius plot of the initial self-heating rates versus inverse temperature. The initial parameters were then optimized by obtaining the lowest χ^2 value. The optimized parameters for eq 7 and (3) were $E_a = 1.28$ eV, $\gamma = 9.93 \times 10^{12}$ min^{-1}, $\alpha_0 = 0.02$, $m = 0.5$, $n = 1$, $p = 0$ and $h/C_{tot} = 61.1$ K (see Table 3 under Grewer). An accurate reproduction of the first process in the thermal decomposition of Li_xCoO_2 in electrolyte is obtained with $\chi^2 = 0.0139$. To confirm that the obtained parameters describe the reaction kinetics well, a comparison of the same model to DSC experiments is needed.

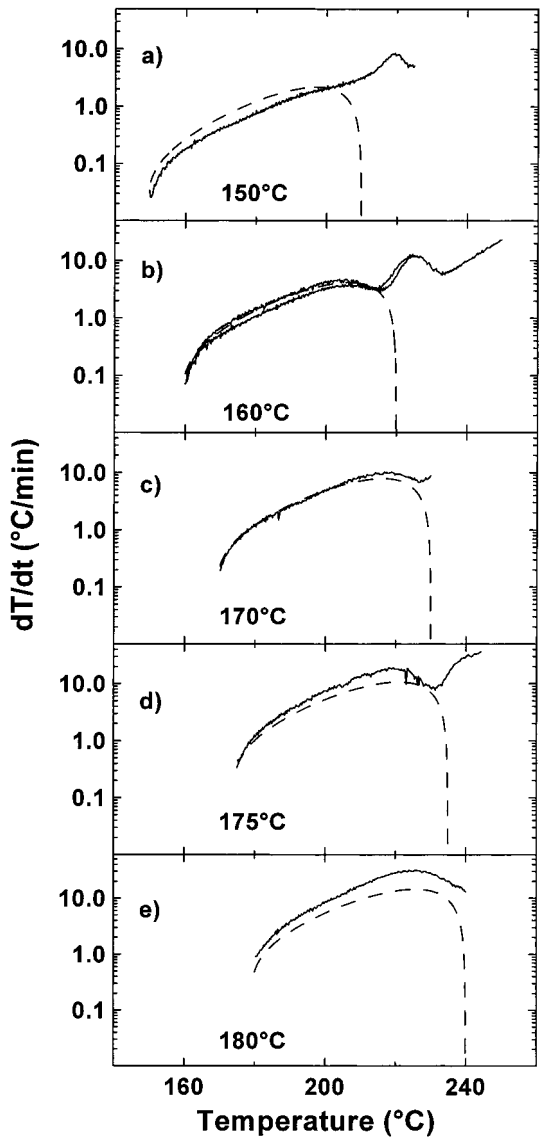

Figure 9. The experiments of Figure 8 (solid) compared to the predictions (dashed) of equations 3 and 7. The parameters used are listed in Table 3 under Grewer. DSC experiments on Li_xCoO_2 in electrolyte at the scan rates indicated.

During the collection of the DSC needed for this work, an interesting feature developed about the reaction of Li_xCoO_2 in electrolyte at elevated temperatures that has not been discussed

TABLE 3: Statistical Analysis

model	E_a (eV)	γ ($\times 10^{13}$) (min^{-1})	m	n	p	α	h/C_{tot} (K)	χ^2_{ARC}	χ^2_{DSC}	χ^2_{Tot}
Grewer	1.284	0.933	0.5	1	0	0.02	61.1	0.0139	0	0.0139
Grewer13	1.291	0.933	0.5	1	0	0.04	70.0	0.0814	0.3829	0.4643
all-fit	1.284	1.48	0.26	1.6	0.49	0.04	66.4	0.0229	0.1027	0.1256
model 11	1.264	0.508	0	1	0.5	0.03	62.3	0.0523	0.3750	0.4273
model 12	1.242	0.400	0	1	2/3	0.03	59.3	0.1810	0.1302	0.3112
model 13	1.262	0.900	0	1	0.75	0.02	58.3	1.9318	0.2267	2.1585
model 14	1.252	1.075	1	1	0	0.04	58.9	0.8812	0.7955	1.6767
Ozawa	1.292									
Kissinger	1.208	0.0749								

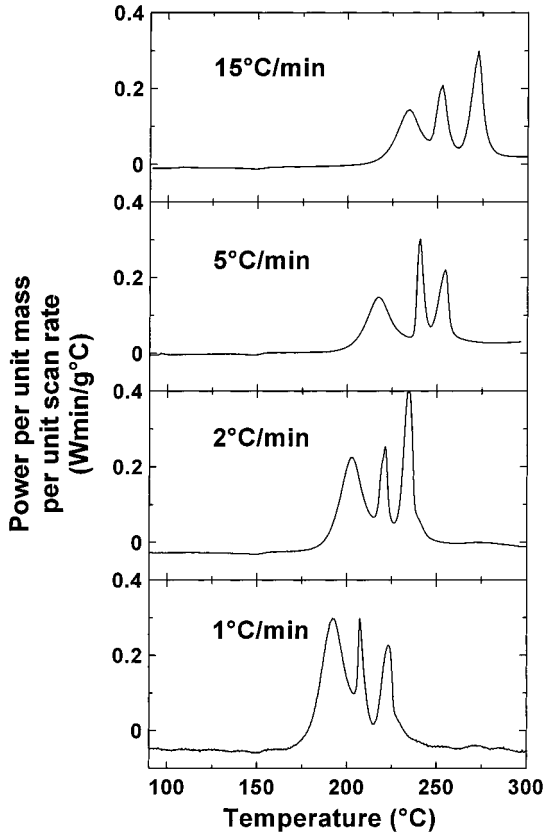

Figure 10. DSC experiments on Li_xCoO_2 charged to 4.2 V in electrolyte, at the heating rates indicated.

in previous work to our knowledge. The DSC profiles of Li_x-CoO_2 charged to 4.2 V at various heating rates are shown in Figure 10. To obtain reproducible DSC traces one must control the analysis conditions strictly, as shown in Figure 11, where we can see the progression from three DSC peaks to a DSC trace with only two peaks. It was believed that the appearance of the two-peak profile was a result of a time-delayed reaction that destroyed the reactant that produced the missing third peak. We set out to systematically discover the nature of this change in DSC pattern. There were three possibilities that were believed to be causing this change to the DSC profile. First, there could be a reaction occurring within the sample upon exposure to the atmosphere in the glovebox. Second, the electrolyte could evaporate, changing the electrolyte-to-powder ratio. For these two possibilities, the obtained profile would be dependent on the time required to produce a DSC sample in the glovebox. The third possibility is that a delayed reaction or evaporation that occurs during the time lapse between fabricating the sample and actual analysis in the calorimeter.

The experimental design to analyze these possibilities was as follows. Prepare three DSC samples from the same electrode at the same time in the glovebox and seal the samples within vials in the glovebox. Next, expose the lightly ground electrode to the atmosphere in the glovebox for various intervals (30, 60, and 120 min.) and prepare three DSC samples at each time interval. One of each of the samples (0, 30, 60, 120 min glovebox exposure) was measured by DSC as soon as possible (day 0 = same day as prepared). A selection of the results are shown in Figure 11, where the DSC profiles contain three peaks even after 120 min exposure to the atmosphere in the glovebox. As the time delay between sample construction and measurement increases, the pattern switches from three peaks to two peaks after about 3 days.

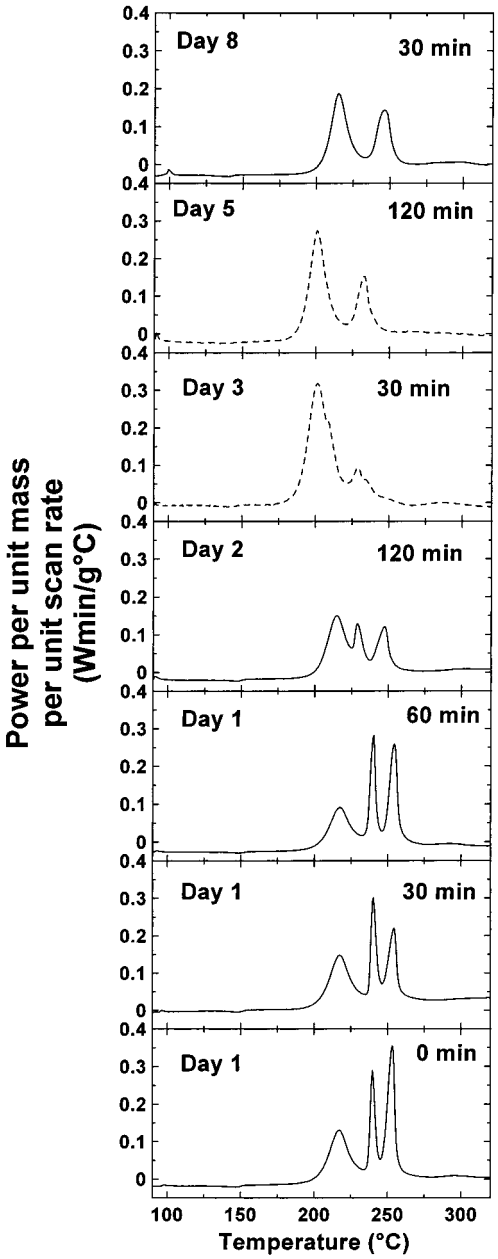

Figure 11. DSC experiments as a function of exposure time of Li_xCoO_2 to glovebox atmosphere (0, 30, 60, 120 min) and as a function of wait time before measurement (given in days), solid curves were measured at 5 K/min, whereas dashed curves at 2 K/min.

The results of this experiment show that the DSC profile of Li_xCoO_2 in electrolyte depends on the time between sample preparation and measurement. Careful procedures are required in order to obtain reproducible results, and we believe that the DSC experiments should be performed on the same day as the sample has been prepared.

The optimized ARC parameters for the Grewer model were then used to calculate DSC profiles for a variety of heating rates. To calculate the DSC response, we need to calculate the reaction power per gram of sample. The power per gram of Li_xCoO_2 is given by eq 6. Using the definition of h in eq 3, we find $H = h/m$, where m is the mass of Li_xCoO_2 in the ARC sample. To obtain h, we use $h/C_{tot} = 61.1$ K, and the heat capacity of an ARC sample. C_{tot} can be calculated from the specific heats, c_i, and masses, m_i, of the materials in the ARC sample. The specific heats of stainless steel, EC and DEC were found in Touloukian et al.[20] and that of Li_xCoO_2 was estimated from the law of

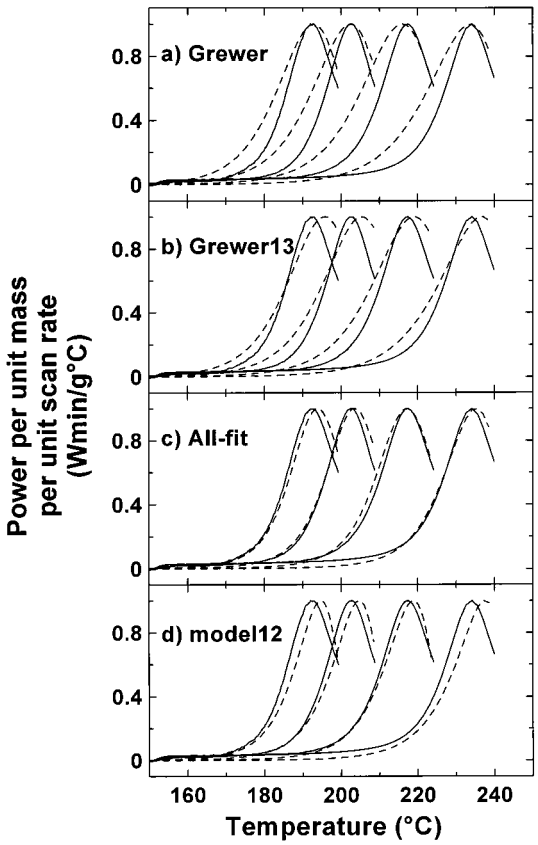

Figure 12. DSC comparisons for various models of the first peak of experimental data (solid) to that of the calculated (dashed) profiles at heating rates of 1,2,5, and 15 K/min. The calculated parameters, with $H = 265$ J/g, corresponding to each panel model are given in Table 3 under their respective models.

Dulong and Petit.[21] For a typical ARC specimen, the heat capacity is about

$$C_{\text{tot}} = \sum_i c_i m_i = 1.0\,\underset{\text{LiCoO}_2}{\frac{\text{J}}{\text{gK}}}\,0.3\text{ g} + \underset{\text{Stainless Steel}}{0.46\,\frac{\text{J}}{\text{gK}}\,0.9\text{ g}} + \underset{\text{Electrolyte}}{1.5\,\frac{\text{J}}{\text{gK}}\,0.4\text{ g}} = 1.3\,\frac{\text{J}}{\text{K}} \qquad (12)$$

where the terms arising from Li_xCoO_2, stainless steel and electrolyte have been indicated (we assume the 0.35 g of wet electrode added is made up of 0.3 g Li_xCoO_2 and 0.05 g of electrolyte). Therefore, $h = 61.1$ K*1.3 J/K = 79 J, and $H = h/0.3\text{ g} \cong 265$ J/g.

Equation 7 is used to calculate $d\alpha/dt$ and eq 6 is used to calculate the evolved power. Figure 12 (panel a, Grewer) shows the model DSC calculation for $H = 265$ J/g, $E_a = 1.28$ eV, $m = 0.5$, $n = 1$, $p = 0$,and $\gamma = 9.93 \times 10^{12}$ min^{-1}, which are the parameters that fit the ARC data well, with a heating rate of 1, 2, 5, and 15 K/min. Also shown is the first peak of the experimental results for Li_xCoO_2 charged to 4.2 V. These plots are presented as normalized curves such that a direct comparison of the peak shapes can be performed and eliminate experimental errors introduced due to the inaccuracy of weighing small amounts (2−7 mg) in the glovebox. The figures only indicate the first exothermic reaction for the experimental data because this is the only reaction that is being modeled with the parameters determined from the ARC. The calculated DSC profiles for the Grewer model do not reproduce well the peak width of the experimental profiles, and this could be due to an incorrect choice for the reaction model ($f(\alpha)$). What remains to be determined is if the addition of optimizing the DSC together with the ARC profiles will result in a kinetic triplet for the Grewer model that can fit the ARC and DSC profiles simultaneously.

The result of optimizing both ARC and DSC profiles simultaneously is shown in Figure 12 (panel b, Grewer13). The parameters to this fit are given in Table 3 under the Grewer13 model, the ARC profiles are not shown, but are similar to those shown in Figure 9. The DSC profiles reproduce the correct shift in peak temperature versus heating rate and have their maxima near the peak in experimental data. The difficulty with these DSC profiles is that an incorrect peak width is obtained; the calculated profiles are much broader than experiment. To sharpen the peak, different reaction models need to be examined.

Equation 7 can be used to reproduce the most common reaction models given in Table 1. It also provides a means of examining other possible reaction schemes through the optimization of its various exponents. The reaction model with the lowest total χ^2 should be indicative of the "true" reaction process for the initial thermal instability of Li_xCoO_2 in electrolyte. This optimization was performed and the values obtained were (see Table 3 under All-fit): $E_a = 1.28$, $\gamma = 1.48 \times 10^{13}$ min^{-1}, $\alpha = 0.04$ (ARC), $m = 0.26$, $n = 1.6$, $p = 0.49$, and $h/C_{\text{tot}} = 66.5$ K with a total χ^2 of 0.1256. The difficulty with this method of kinetic analysis is that no physical or experimental support can be postulated for these exponents. One can obtain remarkably good fits to both ARC (Figure 13) and DSC (Figure 12, panel c All-fit) and as such, these kinetic values can accurately predict other thermal events.

An examination of DSC and ARC profiles for the other models in Table 1 (figures 1−5) shows that the Avrami−Erofeev models (models 11−13) and the Prout−Tompkins model (model 14) can give DSC peaks with about the correct halfwidth, and ARC profiles with the correct temperature dependence. Therefore, we attempted to fit both the ARC and DSC results using these models, and the results are shown in Table 3 under the respective model numbers from Table 1. From this set of reaction models, the kinetic triplet for the thermal decomposition of Li_xCoO_2 in electrolyte at elevated temperatures is best described by an Avrami−Erofeev reaction type (#12) with an activation energy of about 1.24 eV, a frequency factor of 4.0×10^{12} min^{-1} and $\alpha_0 = 0.03$. The calculated ARC (Figure 14) and DSC (Figure 12, panel d model12) profiles are shown and compared to the experiment for this choice of kinetic triplet.

We have found several models that describe the initial reaction of Li_xCoO_2 with electrolyte at elevated temperature reasonably well (Grewer13, All-fit, and model12). However, this kinetic analysis procedure, using both ARC and DSC profiles, eliminates many reaction models quickly and only small refinements to a few models are required to determine an acceptable kinetic triplet. The ARC experiment provides a much higher sensitivity for the process than DSC and thus together, the experiments give a much larger range over which the experiment can be tested and modeled. A higher degree of confidence should be reserved for the parameters that can model both ARC and DSC, which gives the possibility of successful prediction of a variety of thermal events.

There has been a long tradition of determining the kinetic triplet from DSC experiments and two of the famous methods are based on the initial methods proposed by Ozawa[7] and Kissinger.[8] The results of these methods are also shown in Table

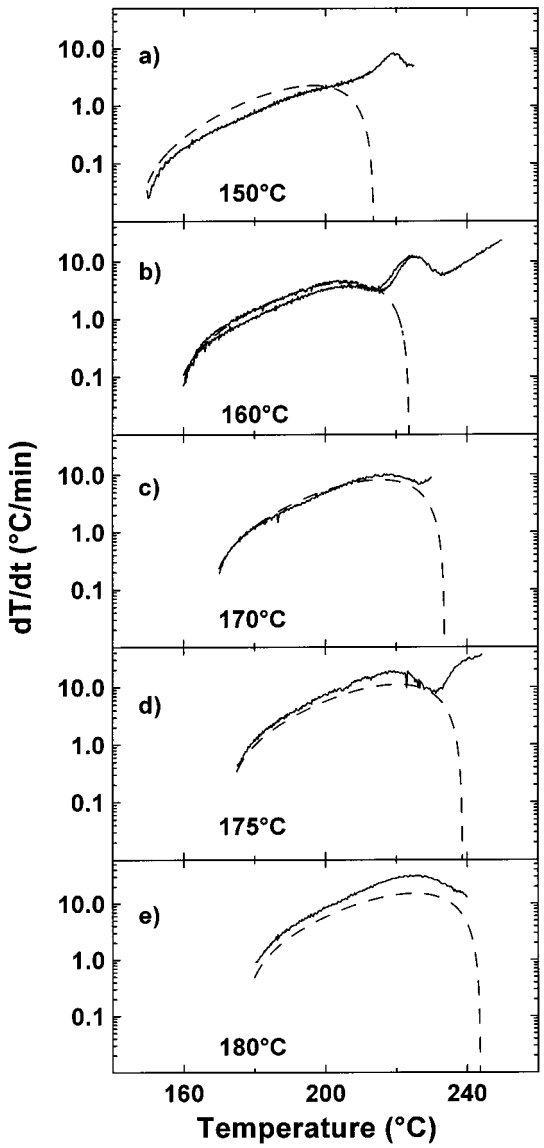

Figure 13. ARC experiments (solid) on Li_xCoO_2 in electrolyte compared to the predictions (dashed) of All-fit model in Table 1 at the start temperature indicated. The parameters are listed in Table 3 under All-fit.

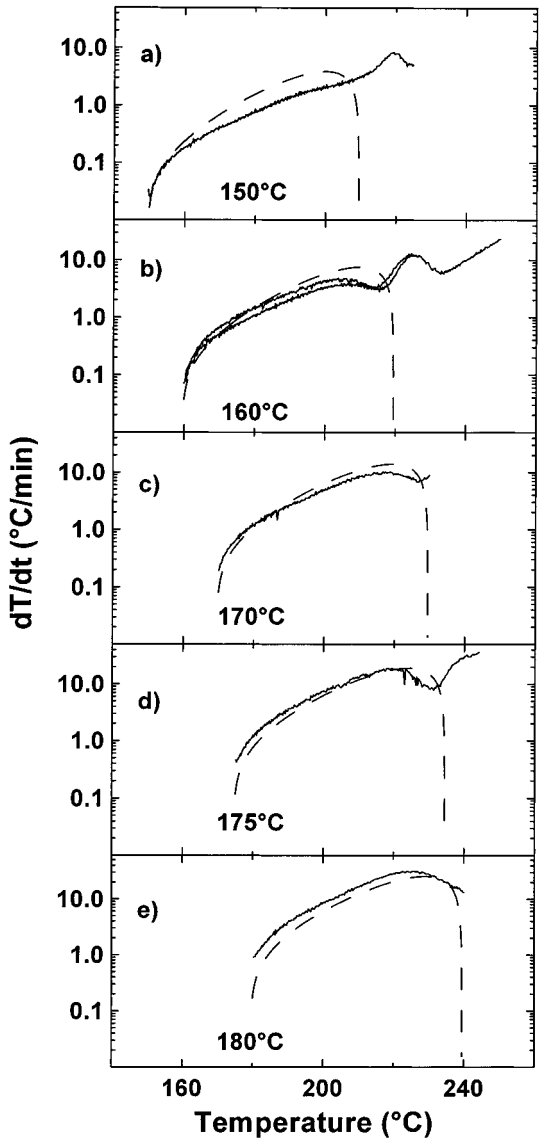

Figure 14. ARC experiments (solid) on Li_xCoO_2 in electrolyte compared to the predictions (dashed) of model 12 model in Table 1 at the start temperature indicated. The parameters are listed in Table 3 under model12.

3. The activation energies obtained are similar to those we found in the fitting described above, although the Kissinger method gives an activation energy that is somewhat low. The methods of Ozawa[7] and Kissinger[8] are useful to give initial estimates for the kinetic parameters, but more detailed analyses with a variety of methods are required in order to obtain full confidence in the kinetic parameters.

Conclusion

The advantages of using both ARC and DSC experiments to obtain reliable determinations of kinetic triplets has been considered and shown. The strong dependence of the ARC profile on the choice of reaction model was clearly demonstrated in Figures 1−5. Therefore, the shape of ARC profile can be used to easily eliminate many possible reaction models. Simultaneous fits to both ARC and DSC results with the same kinetic triplet are possible. Our experiments on Li_xCoO_2 in electrolyte were used to demonstrate the utility of the method and to show that reliable, but perhaps not unique, kinetic triplets can be obtained. The kinetic triplet thus obtained can then be used to predict the outcome of thermal events, for example, in our case those that occur in Li-ion cells under conditions of thermal or electrical abuse.[22,23]

Acknowledgment. The authors thank 3M, 3M Canada Co., and NSERC for funding parts of this work under the Industrial Research Chair Program, and Tim Hatchard for useful discussions.

References and Notes

(1) Brown, W. E.; Dollimore, D.; Galwey, A. K. *Comprehensive Chemical Kinetics* **1980**, *22*, 91.
(2) Popescu, C.; Segal, E. *Int. J. Chem. Kinetics* **1998**, *30*, 313.
(3) Vyazovkin, S.; Wight, C. A. *J. Phys. Chem. A* **1997**, *101*, 8279.
(4) Vyazovkin, S.*Int. J. Chem. Kinetics* **1996**, *28*, 95.
(5) Bohn, M. A.*Thermochim. Acta* **1997**, *337*, 121.
(6) Semper, J.; Nomen, R.; Serra, R.; Gallice, F. *J. Therm. Anal. Cal.* **1999**, *58*, 215.
(7) Ozawa, T. *Bull. Chem. Soc. Jpn.* **1965**, *38*, 1881.
(8) Kissinger, H. E. *Anal. Chem* **1957**, *29*, 1702.
(9) Baider Ceipidor, U.; Brizzi, E.; Bucci, R.; Magri, A. D. *Thermochim. Acta* **1994**, *247*, 347.
(10) Sempere, J.; Nomen, R., Serra, R. *J. Therm. Anal. Cal.* **1999**, *56*, 843.

(11) Underwriter Laboratories Inc., *Standard for Safety 1642—Lithium Batteries*, April **1995**.
(12) Richard, M. N.; Dahn, J. R. *J. Power Sources* **1999**, *79*, 135.
(13) Zhang, Z.; Fouchard, D.; Rea, J. R. *J. Power Sources* **1998**, *70*, 16.
(14) Dahn, J. R.; Fuller, E. W.; Obrovac, M.; von Sacken, U. *Solid State Ionics* **1994**, *69*, 265.
(15) MacNeil, D. D.; Christensen, L.; Landucci, J.; Paulsen, J. M.; Dahn, J. R. *J. Electrochem. Soc.* **2000**, *147*, 970.
(16) Richard, M. N.; Dahn, J. R. *J. Electrochem. Soc*. **1999**, *146*, 2068.
(17) Richard, M. N.; Dahn, J. R. *J. Electrochem. Soc*. **1999**, *146*, 2078.
(18) Townsend, D. I.; Tou, J. C. *Thermochim. Acta* **1980**, *37*, 1.
(19) Grewer, T. *Thermochim. Acta* **1993**, *225*, 165.
(20) Touloukian, Y. S.: Buyco, E. H. *The Thermophysical Properties of Matter − The TPRC Data Series, Volume 5, Specific Heat − Nonmetallic Solids*; Plenum: New York, 1970
(21) Kittel, C. *Introduction to Solid State Physics*, 7th ed.; Wiley and Sons: New York, 1996.
(22) Dahn, J. R.; MacNeil, D. D.; Hatchard, T. Method for Calculating Response of Lithium-Ion Batteries to Thermal, Electrical and Mechanical Abuse. U.S. Patent, application filed.
(23) Hatchard, T.: Dahn, J. R., accepted for publication in *J. Electrochem. Soc.*